Available online at www.sciencedirect.com
SCIENCE DIRECT
Biochimica et Biophysica Acta 1707 (2005) 189–198
BIOCHIMICA ET BIOPHYSICA ACTA
BBA
http://www.elsevier.com/locate/bba

Investigation of B-branch electron transfer by femtosecond time resolved spectroscopy in a *Rhodobacter sphaeroides* reaction centre that lacks the Q_A ubiquinone

Dmitrij Frolov[a,*], Marion C. Wakeham[b], Elena G. Andrizhiyevskaya[a], Michael R. Jones[b], Rienk van Grondelle[a]

[a]*Department of Physics and Astronomy, Free University of Amsterdam, De Boelelaan 1081, 1081 HV, Amsterdam, The Netherlands*
[b]*Department of Biochemistry, School of Medical Sciences, University of Bristol, University Walk Bristol, BS8 1TD, United Kingdom*

Received 11 October 2004; received in revised form 30 November 2004; accepted 1 December 2004
Available online 4 January 2005

Abstract

The dynamics of electron transfer in a membrane-bound *Rhodobacter sphaeroides* reaction centre containing a combination of four mutations were investigated by transient absorption spectroscopy. The reaction centre, named WAAH, has a mutation that causes the reaction centre to assemble without a Q_A ubiquinone (Ala M260 to Trp), a mutation that causes the replacement of the H_A bacteriopheophytin with a bacteriochlorophyll (Leu M214 to His) and two mutations that remove acidic groups close to the Q_B ubiquinone (Glu L212 to Ala and Asp L213 to Ala). Previous work has shown that the Q_B ubiquinone is reduced by electron transfer along the so-called inactive cofactor branch (B-branch) in the WAAH reaction centre (M.C. Wakeham, M.G. Goodwin, C. McKibbin, M.R. Jones, Photo-accumulation of the $P^+Q_B^-$ radical pair state in purple bacterial reaction centres that lack the Q_A ubiquinone, FEBS Letters 540 (2003) 234–240). In the present study the dynamics of electron transfer in the membrane-bound WAAH reaction centre were studied by femtosecond transient absorption spectroscopy, and the data analysed using a compartmental model. The analysis indicates that the yield of Q_B reduction via the B-branch is approximately 8% in the WAAH reaction centre, consistent with results from millisecond time-scale kinetic spectroscopy. Possible contributions to this yield of the constituent mutations in the WAAH reaction centre and the membrane environment of the complex are discussed.

Keywords: Reaction centre; Electron transfer; B-branch; Mutagenesis; Compartmental analysis; Femtosecond spectroscopy

1. Introduction

In the reaction centres of purple bacteria, light energy is used to drive the transfer of an electron from a pair of bacteriochlorophylls (BChls) located close to the periplasmic side of the membrane, to a quinone located close to the cytoplasmic side. This triggers a cycle of electron flow that is coupled to the generation of an electrochemical gradient of protons across the bacterial cytoplasmic membrane.

Perhaps the most heavily studied purple bacterial reaction centre is that from *Rhodobacter sphaeroides*. This complex is composed of the H, L and M polypeptides and ten cofactors. The latter comprise four molecules of BChl, two molecules of bacteriopheophytin (BPhe), two molecules of ubiquinone, a single photoprotective carotenoid and a non-heme iron atom (Fig. 1A). The L- and M-polypeptides form a heterodimeric protein scaffold that encases the BChl, BPhe and ubiquinone cofactors [1–4], and the latter are arranged in two membrane-spanning branches, termed A (active) and B (inactive), around an axis of two-fold

Abbreviations: B_A,B_B, A- and B-branch accessory bacteriochlorophyll; BChl, bacteriochlorophyll; BPhe, bacteriopheophytin; DADS, decay associated difference spectra; FTIR, Fourier transform infrared; H_A,H_B, A- and B-branch bacteriopheophytin; P, primary electron donor; Q_A,Q_B, A- and B-branch ubiquinone; Rb., Rhodobacter

* Corresponding author. Tel.: +31 20 5987932; fax: +31 20 5987999.
E-mail address: dmitrij@nat.vu.nl (D. Frolov).

0005-2728/$ - see front matter © 2004 Elsevier B.V. All rights reserved.
doi:10.1016/j.bbabio.2004.12.006

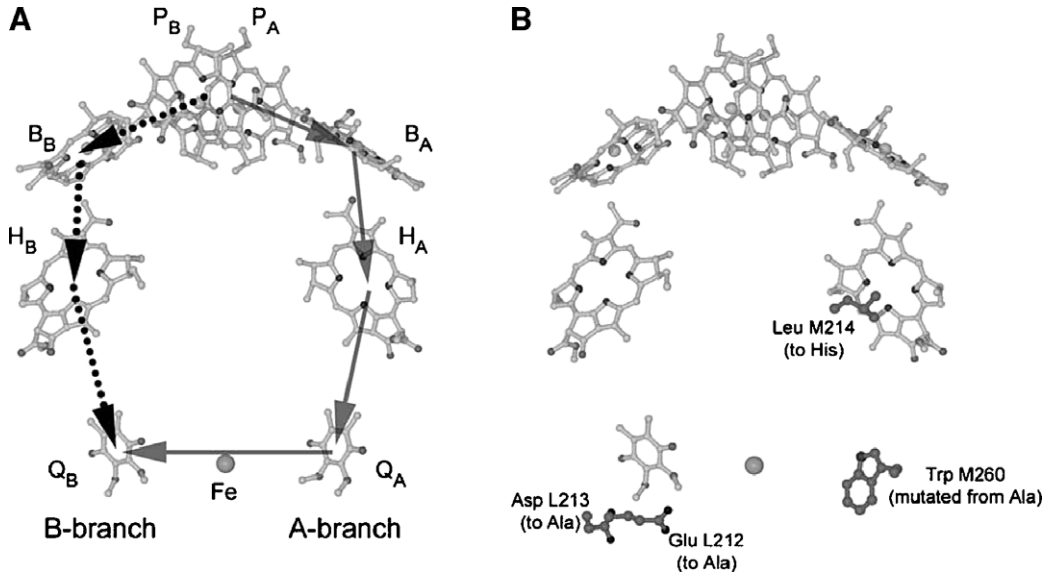

Fig. 1. Structural models showing (A) cofactor organisation in the wild-type reaction centre and (B) the AM260W reaction centre (Protein Data Bank entry 1QOV [49]) with the other residues that were mutated to form the WAAH reaction centre highlighted. In (A), the route of A-branch and B-branch electron transfer is indicated by the solid and dotted arrows, respectively.

symmetry that connects the P_A and P_B BChls with the non-heme iron (Fe in Fig. 1A) [2–5]. In the initial steps of energy transduction, light energy drives the transfer of an electron along the A-branch of cofactors [6] from the "special pair" of excitonically-coupled BChl molecules (P) to the Q_A ubiquinone [7–12]. This transmembrane electron transfer takes place on a picosecond time-scale, and involves the intervening monomeric BChl (B_A) and BPhe (H_A) [7–12]. The electron residing on the Q_A ubiquinone is passed to the Q_B cofactor binding site, where a loosely-bound ubiquinone is reduced to the ubisemiquinone [13,14]. A second light-driven transmembrane electron transfer results in further reduction and double protonation of the Q_B ubisemiquinone to form ubiquinol [13,14].

Several research groups have addressed the issue of the strong asymmetry of electron transfer in the purple bacterial reaction centre, using both experimental and computational approaches, and a number of contributory factors have been proposed. These include asymmetry in electronic coupling between cofactors on the A- and B-branches, attributed in some studies to small differences in the spacing of cofactors on the two branches [15–23], asymmetry in the dielectric environment on the two branches [24,25] and asymmetry in static intra-protein electric fields [26]. A much-discussed idea is that asymmetric electron transfer is largely attributable to a difference in energy between the $P^+B_A^-$ state and the analogous $P^+B_B^-$ state, with the latter having a significantly higher free energy than either $P^+B_A^-$ or P* does [27–31]. In recent years there has also been considerable interest in the use of mutagenesis to re-route electron transfer along the normally inactive B-branch [32–47].

One of the challenges of this topic is discriminating between A- and B-branch electron transfer in a structure where the cofactors at each position along the A- and B-branches are chemically identical, and are separated by similar distances. The two reaction centre BPhes, for example, have almost identical absorbance spectra at room temperature. Protein engineering has been used to address this problem by changing the cofactor composition of the A-branch. Mutagenesis of Leu M214 to His (LM214H) causes the reaction centre to assemble with a BChl rather than BPhe at the H_A position A-branch [32]. The new A-branch BChl, termed β_A, has a Q_y absorbance significantly to the red of that of the remaining H_B BPhe on the B-branch, and has a significantly lower redox potential [32]. The LM214H single mutant reaction centre has a slowed rate of primary electron transfer to a state that has a mixed $P^+B_A^-/P^+\beta_A^-$ character [32] (referred to henceforth as $P^+I_A^-$). The LM214H reaction centre also has a slowed rate of secondary electron transfer from $P^+\beta_A^-$ to $P^+Q_A^-$ (from 200 ps^{-1} to 600 ps^{-1}), and a decreased yield of electron transfer to Q_A (from ~100% to ~60%) [32]. The 40% decrease in the yield of the $P^+Q_A^-$ state is due to competition from an accelerated rate of decay of the mixed $P^+I_A^-$ state to the ground state (0.9 ns^{-1} compared with 20 ns^{-1} for the decay of $P^+H_A^-$ in the wild-type) [32]. The mutation has provided insights into the design of the reaction centre, particularly the purpose of the specialist BPhe cofactor, and importantly also allows absorbance changes associated with the reduction of the H_B BPhe to be discriminated [32,33]. It has been proposed on kinetic grounds that the LM214H mutant forms the $P^+H_B^-$ state with a yield of a few percent (estimated at between 3% and 8% [33,41]), and spectroscopic data has been presented in support of this [33,41].

A second strategy that has been used is to sterically exclude the Q_A ubiquinone from the *R. sphaeroides* reaction

centre through the mutation of Ala M260 to Trp (AM260W). A combination of spectroscopy and X-ray crystallography has shown that this mutation prevents the incorporation of the Q_A ubiquinone during assembly (Fig. 1B), and blocks electron transfer along the A-branch beyond the H_A cofactor [48,49]. The AM260W mutation isolates the Q_B cofactor as the only reaction centre ubiquinone, and drastically shortens the lifetime of the radical pair that is the end product of A-branch electron transfer, from approximately 100 ms for $P^+Q_B^-$ in the wild-type complex to approximately 10 ns for $P^+H_B^-$ in the absence of Q_A in the AM260W reaction centre [48].

In a recent report, it was concluded that a reaction centre in which the AM260W, LM214H and a double Glu L212 to Ala/Asp L213 to Ala (EL212A/DL213A) mutation were combined (Fig. 1B) formed the radical pair $P^+Q_B^-$ by B-branch electron transfer following flash excitation [45]. The EL212A/DL213A double mutation makes the binding pocket of the Q_B ubiquinone less polar [50–52], and prevents further reduction of Q_B beyond the semiquinone state [50]. The $P^+Q_B^-$ radical pair could be photo-accumulated by a train of excitation flashes in this quadruple mutant (termed WAAH), and was detected by monitoring absorbance changes indicative of photo-oxidation of the P BChls that persisted on a millisecond time-scale [45]. In the absence of the Q_A ubiquinone, the detection of a P^+-containing state on this time-scale indicated the formation of the $P^+Q_B^-$ radical pair (as the longest-lived radical pair states involving P^+ and either A- or B-branch BChl or BPhe anions are expected to decay on a time-scale of, at most, a few nanoseconds). This state was formed with a yield of approximately 17% following excitation with a single, low-intensity actinic flash of red light with a duration of 6 μs (half-peak width) [45]. The formation of $P^+Q_B^-$ by B-branch electron transfer in the WAAH reaction centre was subsequently confirmed by FTIR spectroscopy [46,47].

The experiments involving millisecond time-scale transient absorbance spectroscopy outlined above have the advantage that, with the type of Q_A-deficient mutant reaction centres being studied, they produce absorbance changes that can be straightforwardly attributed to the formation of $P^+Q_B^-$ by B-branch electron transfer. However, the nature of the excitation flash used means that the measurement does not allow the calculation of a yield of B-branch electron transfer under genuine single turnover conditions. In the present report, we have used absorbance difference spectroscopy with femtosecond time-scale excitation and measuring pulses to monitor electron transfer in the WAAH mutant reaction centre, and have analysed the resulting data using a compartmental model in order to estimate the yield of $P^+Q_B^-$ formed by B-branch electron transfer in the WAAH reaction centre. The findings are compared with new results from millisecond time-scale single wavelength kinetic spectroscopy.

2. Materials and methods

2.1. Biological material

The construction of the WAAH mutant reaction centre has been described previously [45]. It contains the mutations Leu M214 to His (LM214H), Ala M260 to Trp (AM260W), Glu L212 to Ala (EL212A) and Asp L213 to Ala (DL213A). The positions of these mutations are shown in Fig. 1B. Reaction centre *pufLM* genes containing these mutations were expressed in *R. sphaeroides* deletion strain DD13 [53], using a derivative of expression vector pRKEH10D that lacks the *pufBA* genes that encode the core LH1 antenna complex [53]. This produced transconjugant strains that had mutant reaction centres but lacked both types of light-harvesting complex.

Experimental material consisted of intracytoplasmic membrane fragments prepared from antenna-deficient cells that had been grown under semiaerobic conditions in the dark, using procedures described previously [54].

2.2. Steady state and time resolved spectroscopy

Absorbance spectra of intracytoplasmic membranes diluted in 20 mM Tris HCl (pH 8.0) were recorded using a Perkin Elmer UV-VIS double beam spectrophotometer.

Femtosecond transient absorbance difference spectra were recorded using antenna-deficient membranes diluted in 20 mM Tris HCl (pH 8.0), and a spectrometer that has been described previously [55,56]. In brief, the output of a Ti:Sapphire oscillator was amplified by means of chirped pulse amplification (Alpha-1000 US, B.M. Industries) generating 1 kHz, 795 nm, 60 fs pulses. The absorption of the sample was 0.6 OD mm^{-1} at 795 nm, and typically 20% of the reaction centres were excited with each pulse. Transient absorption spectra were collected with probe and excitation beams oriented at the magic angle. The steady state absorption spectrum of the sample before and after measurements did not show any changes. Spectra were corrected for white light group velocity dispersion and instrument response function, and fitted globally with five components as described previously [57].

Millisecond (ms) time-scale transient absorption was recorded using a single beam spectrophotometer of local design, as described in detail recently [45]. In order to ensure full dark adaptation of the sample, the measuring beam was switched on only 50 ms before recording commenced, and during dark periods the photomultiplier was provided with light from a light-emitting diode of an intensity equal to that of the measuring beam. Excitation was provided by a frequency doubled Nd-YAG laser (Spectron Ltd., Rugby, U.K) which produced 10 ns pulses of light at 532 nm with energy in excess of 100 mJ/pulse The photomultiplier was protected with a 580 nm cut-off filter, and BG39 and 530 nm cut-on filters. The amplifier time constant was 100 μs, the

dark time between flashes was 30 s, and 8 transients were signal-averaged to produce the final result.

Samples were housed in a glass cuvette with an optical path length of 1 cm, and consisted of antenna-deficient membranes diluted in 20 mM Tris HCl (pH 8.0). Sodium ascorbate was added to a final concentration of 300 μM to ensure that there was no pre-oxidation of the P BChls. For the purposes of comparison of different samples, in all experiments, intracytoplasmic membranes were diluted to a reaction centre concentration of approximately 1 μM, and data were normalised as described recently [45]. Briefly, after each experiment the absorbance spectrum of the sample was measured, corrected for background scatter, and the amplitude of the P Q_y band was recorded. This amplitude was then used to normalise the amplitude of the transient absorbance traces.

3. Results and discussion

3.1. Steady state spectroscopy

The Q_y regions of the absorbance spectra of membrane-bound wild-type and WAAH mutant reaction centres are compared in Fig. 2. For the wild-type reaction centre the band at 757 nm is attributable to the reaction centre BPhes (termed the H Q_y band), the band at 804 nm is attributable to the accessory BChls with a smaller contribution from the P BChls (termed the B Q_y band), whilst the band at 869 nm is attributable to the P BChls (termed the P Q_y band).

The major change in the absorbance spectrum of the WAAH mutant was a decrease in the intensity of the H Q_y band and the appearance of additional absorbance between the H Q_y band and the B Q_y band. The maximum of the B Q_y band is also shifted to shorter wavelengths by 1 nm. These changes arise from the replacement of the H_A BPhe by a BChl, brought about by the LM214H mutation [32]. There was also a 4 nm blue-shift of the maximum of the P Q_y band in the spectrum of the WAAH mutant, that has previously been attributed to the AM260W mutation [48].

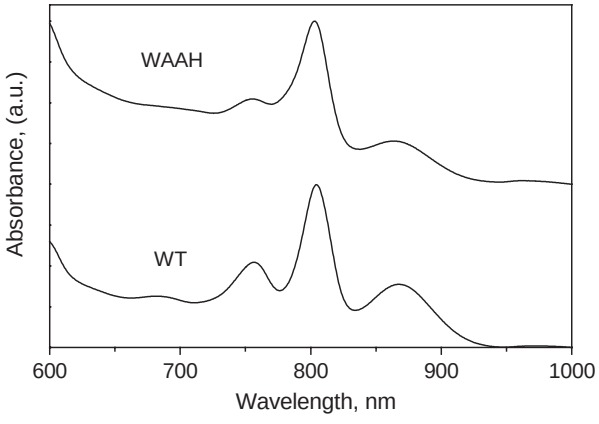

Fig. 2. Steady state absorbance spectra of mutant and wild-type (WT) reaction centres at room temperature.

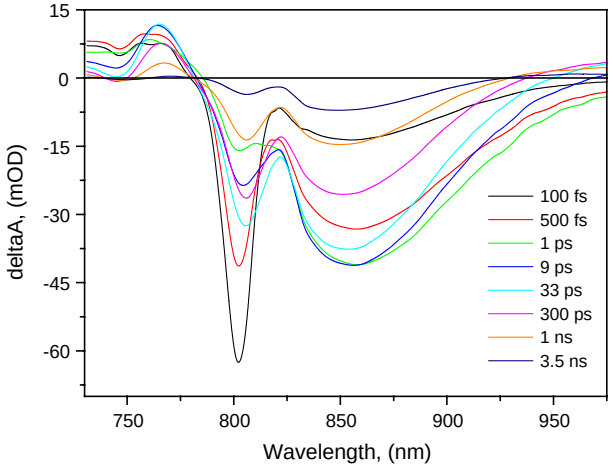

Fig. 3. Transient absorbance difference spectra at room temperature obtained at various times after the excitation of membrane-bound WAAH reaction centres with a 60 fs excitation pulse centred at 795 nm.

3.2. Femtosecond absorbance difference spectroscopy

Absorbance difference spectra were obtained at varying time intervals after a 795 nm excitation pulse, with a maximum delay time of 4 ns. Representative spectra recorded at several delay times are shown in Fig. 3. The 795 nm pulse mainly excited B_A, with the possibility of some excitation of B_B and β_A. Excitation caused a bleach around 800 nm at early delay times (100 fs spectrum, Fig. 3), and subsequent rapid excitation transfer from the monomeric BChls to P caused a bleaching of P band around 870 nm, concomitant with a loss of the bleach at 800 nm (500 fs spectrum, Fig. 3). Stimulated emission on the red side of the bleach of the 870 nm P band was maximal at around 1 ps, and subsequently decayed as the P* state decayed through electron transfer or emisson (1 ps spectrum compared with 33 ps spectrum, Fig. 3).

A global analysis of the data was carried out using locally written software as described previously [57]. Five spectrally- and temporally-distinct components were needed to describe the data, and the decay associated difference spectra (DADS) of these components are shown in Fig. 4.

The first DADS (Fig. 4, solid line) had a lifetime of 270 fs, and is attributed to the short-lived excited states of the monomeric BChls (mostly B_A*) and energy transfer from the monomeric BChls to P. The next DADS (Fig. 4, dashed line), with the lifetime of 8.3 ps, is attributed mainly to the decay of P* to the $P^+I_A^-$ state. This lifetime was similar to the 6 ps lifetime determined previously for reaction centres with the LM214H mutation [41]. Given that it has been shown that electron transfer can also be driven by B_A* in wild-type reaction centres [58], it is also possible that there was a contribution of a small amount of $P^+B_A^-$ and/or $B_A^+H_A^-$ to this spectrum. The third DADS (Fig. 4, dotted line), with the

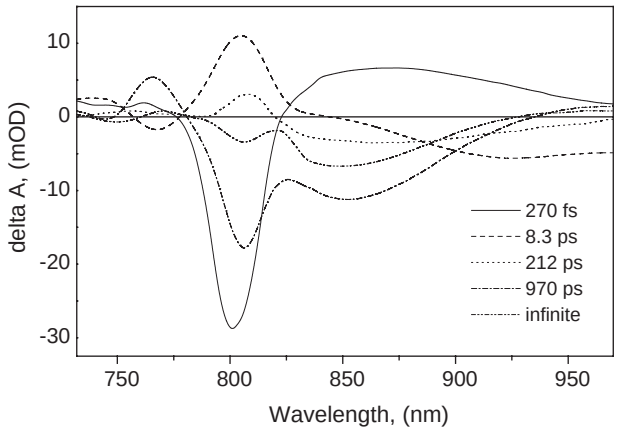

Fig. 4. Decay associated absorption difference spectra of membrane-bound WAAH reaction centres. The 270 fs and infinite spectra were multiplied by 0.25 and 2, respectively, for the purposes of comparison.

lifetime of 212 ps, is probably attributable to a combination of electron transfer via the B-branch and changes in the $P^+I_A^-$ state. In the latter case this does not involve forward electron transfer to Q_A, as this cofactor is absent in the WAAH mutant. The fourth DADS (Fig. 4, dot-dash line), with the lifetime of 970 ps, is attributed to the overall decay of the $P^+I_A^-$ state, which is known to occur with a lifetime of 0.9 ns in purified reaction centres with the LM214H mutation [41]. The fifth DADS (Fig. 4, dash-dot-dot line) had a lifetime that was infinite on the time-scale of our experiments (4 ns), and had a shape usually observed for the P^+I^- state. Given the long lifetime of this state we ascribe it to a mixture of $P^+H_B^-$ and $P^+Q_B^-$. The lifetime for forward electron transfer from $P^+H_B^-$ to $P^+Q_B^-$ has been estimated to be between 2 and 12 ns [59], consistent with our assignment. This reaction is at least 10-fold slower than the equivalent $P^+H_A^-$ to $P^+Q_A^-$ reaction in wild-type reaction centres.

3.3. Modelling of electron transfer in the WAAH mutant

Further analysis of the time-resolved absorbance difference spectra was carried out using the simple kinetic model shown in Fig. 5A, which was described by a system of linear differential equations. The model assumes that

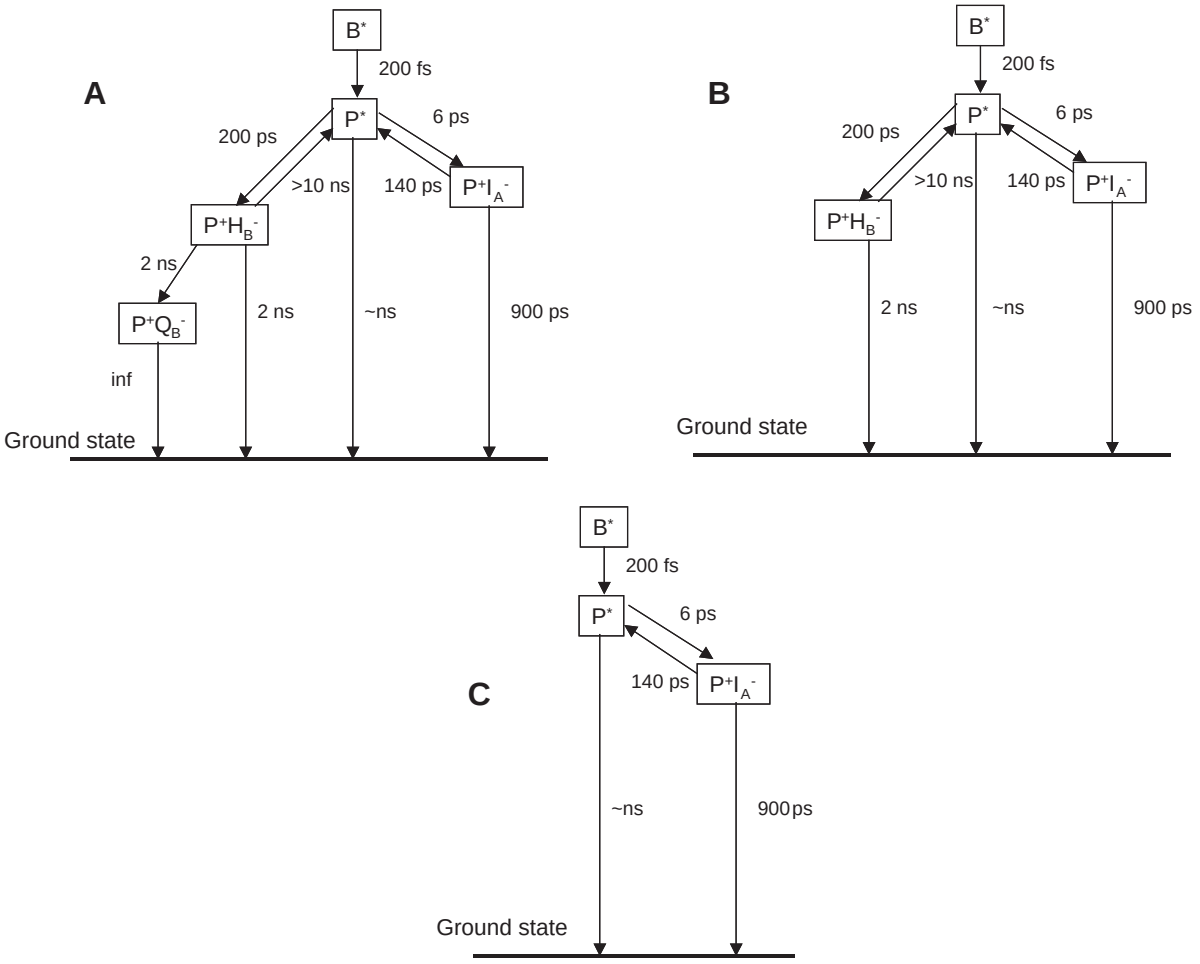

Fig. 5. Compartmental models of electron transfer used in data modelling. Model (A) assumes branched electron transfer to P^+I^- via the A-branch or $P^+Q_B^-$ via the B-branch. Model (B) is a derivative of (A) that assumes that there is no electron transfer from H_B to Q_B. Model (C) is a further derivative that assumes no B-branch electron transfer.

both A- and B-branch electron transfer occur in the WAAH reaction centre, consistent with previous observations from transient absorbance spectroscopy and FTIR difference spectroscopy [45–48]. The model incorporates reported lifetimes of different states in *R. sphaeroides* reaction centres containing the LM214H mutation, and takes into account known values for the analogous *R. capsulatus* LM212H mutant reaction centres. It also assumes that the Q_A-excluding AM260W mutation completely prevents forward electron transfer from H_A^- to Q_B, and does not affect the kinetics of electron transfer along the remaining part of the A-branch. Both of these assumptions are in accord with previous spectroscopic studies of the AM260W mutant [48].

In setting time constants for individual reactions, the LM214H mutation is known to slow the time constant for the $P^*\rightarrow P^+I_A^-$ charge separation step to 6 ps [41]. Studies of reaction centres with LM214H mutation have also shown that the lifetime of the $P^+I_A^-$ state decreases to 0.9 ns [32,41] compared to 10–20 ns in the wild-type reaction centre.

For the B-branch reactions, it has been proposed that the $P^*\rightarrow P^+H_B^-$ charge separation step in LM214H reaction centres proceeds with a time constant of 200 ps [41], and accordingly this time constant was used in the model. The $P^+H_B^-\rightarrow P^+Q_B^-$ transfer time has been estimated to be in the range 2–12 ns [59], considerably longer than the equivalent $P^+H_A^-\rightarrow P^+Q_A^-$ transfer time [40]. In the present model the lower limit of 2 ns was used. Although a time constant of 4–8 ns has been estimated for the $P^+H_B^-\rightarrow PH_B$ recombination reaction in *R. capsulatus* reaction centres [59], a better fit of the data was obtained using a value of 2 ns.

Reverse electron transfer reactions in the model were connected with forward electron transfer via a Boltzman distribution; thus $k_{reverse}=k_{forward}*\exp(-\Delta/kT)$, where Δ is the energy difference between the states, T is absolute temperature and k is the Boltzman constant. The free energy difference between the P* and $P^+I_A^-$ state in reaction centres with LM214H mutation has been estimated to be in the range 50–100 meV [41], and a value of 80 meV was used. The free energy difference between the P* and $P^+H_B^-$ states is not known for certain, however it is expected to be around the level of ≤150 meV [36]. A value of 100 meV was used, which gave effectively the same yield of $P^+Q_B^-$ as when a value of 150 meV was used. A free energy difference of 100 meV resulted in >10 ns transfer time for the $P^+H_B^-\rightarrow P^*$ process, which has a very low yield.

In order to exclude the influence of apparatus functions on the experimentally measured kinetics, a common kinetic curve was constructed from the data obtained from global analysis by integrating over all wavelengths in the data set. This common kinetics curve to the first approximation shows the dynamics of all populations of the spectral forms that exist in the data set. In Fig. 6A this curve is compared with the theoretical curves calculated from the model shown in Fig. 5A. A good fit was obtained using

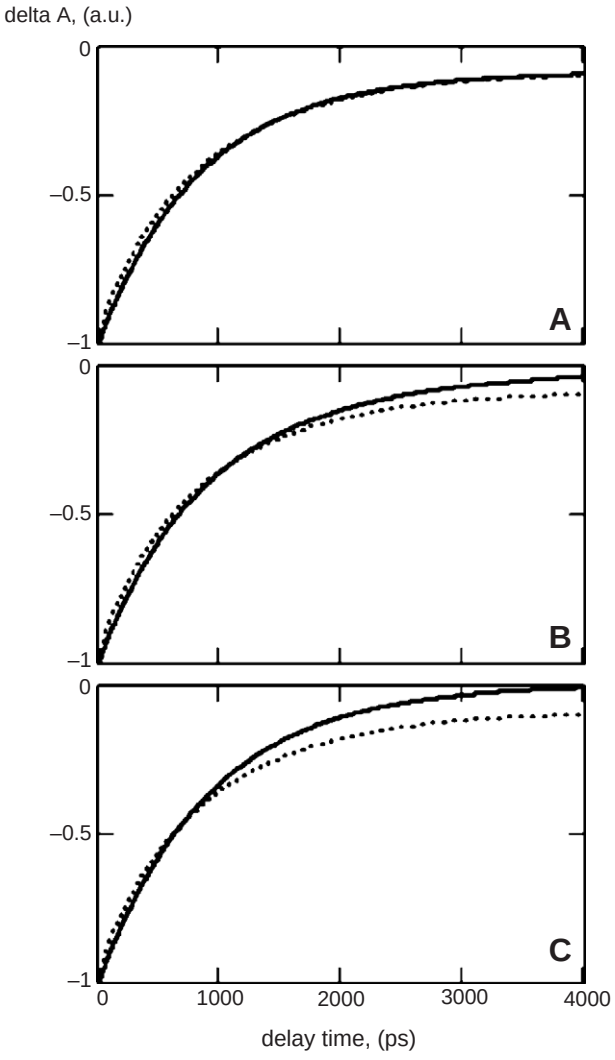

Fig. 6. Integrated delta absorption signal (dash) together with the fit (solid) obtained on the basis of the compartmental models shown in Fig. 5A, B and C, respectively.

the parameters described in Fig. 5A, and gave a yield of 8±1% for the $P^+Q_B^-$ state formed by B-branch electron transfer.

To test the robustness of this model the data was also fitted using models which did not involve electron transfer from H_B to Q_B (Fig. 5B), and which involved only A-branch electron transfer (Fig. 5C). Both of these variants gave a significantly worse fit compared with the model that involved electron transfer along the B-branch to the $P^+Q_B^-$ state (Fig. 6B and C compared with A).

The population traces of the different states in the model in Fig. 5A are shown in Fig. 7, with the dynamics at early times shown on an expanded scale (inset). These data were used to link the transient absorption spectra in Fig. 3 to the different states (species). Thus the B* state formed by the excitation pulse gives rise to the 100 fs spectrum in Fig. 3, and this is followed by very fast transfer to the P* state, which in this model should have the highest contribution to the transient absorption signal at

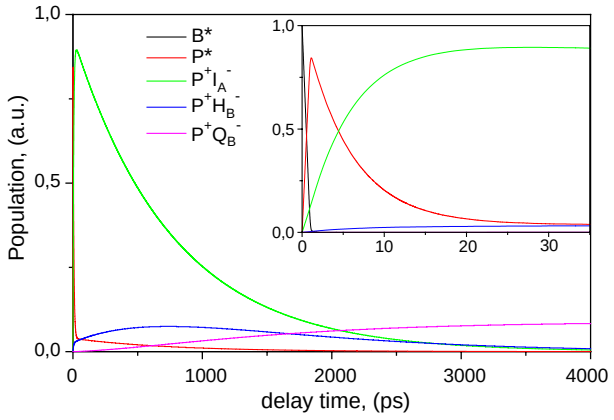

Fig. 7. Population dynamics for each species in the model in Fig. 5A. The inset shows the dynamics during the first 35 ps on an expanded scale.

around 1 ps. The 9 ps spectrum in Fig. 3 is contributed to by $P^+I_A^-$ (73%), P* (24%) and $P^+H_B^-$ (2%), and around 1% of the initial population is lost, mainly as stimulated emission from P*. At 33 ps the transient absorbance spectrum of the $P^+I_A^-$ state dominates the time resolved data (see inset to Fig. 7), whilst the 300 ps transient absorbance spectrum consists of mainly $P^+I_A^-$ with a smaller contribution from $P^+H_B^-$. Finally, the 3.5 ns transient absorption spectrum is mostly due to $P^+Q_B^-$ although, from the shape of the spectrum, it seems possible that there is also some contribution from the reaction centre triplet state, which is manifested as the overall bleaching of reaction centre absorbance.

3.4. Millisecond time-scale transient absorbance spectroscopy

The multi-wavelength transient absorbance measurements described in Figs. 3 and 4 have the advantage that they employ femtosecond time-scale excitation pulses, and so enable the single turnover yield of B-branch electron transfer to $P^+Q_B^-$ in the WAAH reaction centre to be determined. They have the disadvantage that the yield of $P^+Q_B^-$ is determined indirectly from the modelling of the data. On the other hand, the millisecond time-scale single-wavelength transient absorbance measurements on the WAAH reaction centre described previously [45] provide an unambiguous and direct measurement of the yield of flash-induced $P^+Q_B^-$ formed by B-branch electron transfer, and provide a simple and rapid method for assessing the impact of additional mutations on this yield. However, this measurement has the disadvantage that excitation is provided by a weak, temporally broad (~6 μs) excitation pulse, which raises the possibility of multiple excitation of the reaction centre. It is therefore problematic to relate the 8% yield of $P^+Q_B^-$ estimated above with the 17% yield of $P^+Q_B^-$ determined previously [45].

To bridge the gap between the two types of measurement, single wavelength transient absorbance spectroscopy employing excitation pulses of a few nanoseconds duration was applied to membrane-bound wild-type and WAAH reaction centres. Fig. 8 shows P^+ formation in antenna-deficient membranes containing wild-type reaction centres, measured by monitoring the absorbance changes at 542 nm [60,61] elicited by a train of 10 actinic light pulses delivered by a laser operating at 532 nm (see Materials and methods). Each pulse was saturating, but the pulse length (~10 ns) was approximately 10^3 shorter than that used in previous experiments with a xenon flash-lamp [45]. This placed the length of the excitation pulse much closer to the expected ~0.9 ns lifetime of the mixed $P^+I_A^-$ state formed by A-branch electron transfer in the WH and WAAH reaction centres [41].

As can be seen from Fig. 8, the flash train caused full photo-oxidation of P in the wild-type reaction centres, the signal decaying during the dark time between flashes with a lifetime of hundreds of milliseconds. The addition of stigmatellin produced an acceleration in the rate of decay of the P^+ signal, but the initial photo-oxidation was not affected (data not shown). As discussed in detail recently [45], this pattern is consistent with that expected when flash excitation produces a mixed $P^+Q_A^-/P^+Q_B^-$ state (P^+Q^-), and when the formation of Q_B^- is blocked by stigmatellin. The rate of decay of the P^+Q^- state was not analysed, as the experiments were carried out in the presence of ~300 μM sodium ascorbate to ensure that the P BChls were fully reduced in the dark between flash trains, which has the potential to make the decay of the P^+ transient artificially fast. The absorbance transient was similar to that obtained in

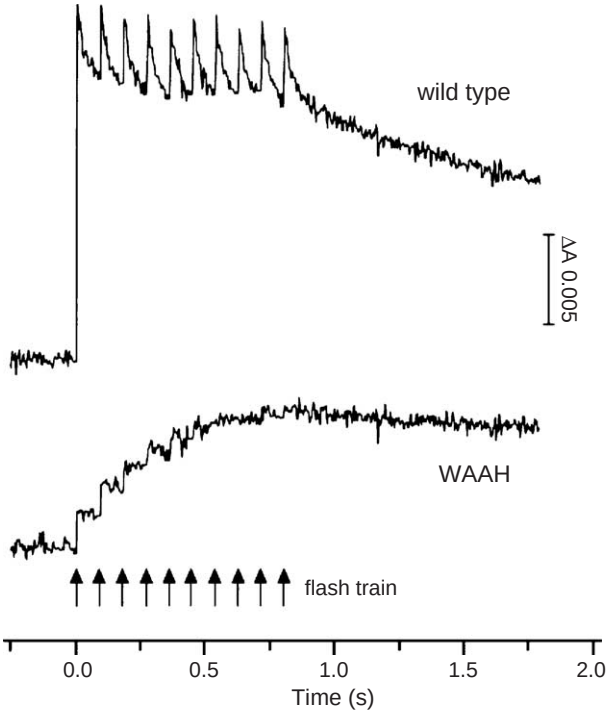

Fig. 8. P^+ formation in antenna-deficient membranes containing either wild-type or WAAH mutant reaction centres, elicited by excitation from 10 laser flashes at room temperature.

previous studies using xenon flash excitation of membrane-bound wild-type reaction centres.

Also shown in Fig. 8 is data recorded for antenna-deficient membranes containing WAAH mutant reaction centres, normalised as described in Materials and methods. Membranes containing reaction centres with the WAAH mutation also showed evidence of the formation of a P^+-containing state. As discussed in detail recently the millisecond life-time of this state, its sensitivity to stigmatellin (not shown), and the lack of a Q_A ubiquinone in the WAAH reaction centre provide good evidence that it is $P^+Q_B^-$, formed by electron transfer along the B-branch of cofactors [45]. The yield of $P^+Q_B^-$ was approximately 10% on the first flash, and the state was photo-accumulated on subsequent flashes. This pattern was similar to that reported previously using xenon flash excitation of the membrane-bound WAAH reaction centres [45], but the yield was reduced (from 17% to 10% on the first flash, and from 47% to 41% after 10 flashes).

3.5. The extent of B-branch electron transfer to Q_B in the WAAH reaction centre

From the analysis of the experimental data presented in Fig. 3 we estimate that the excitation of membrane-bound WAAH mutant reaction centres at 795 nm with a 60 fs laser flash produces an 8% yield of the $P^+Q_B^-$ radical pair, formed by B-branch electron transfer. This yield is similar to the 10% yield estimated from single wavelength millisecond time-scale measurements employing an excitation pulse of a few nanoseconds duration. This similarity validates the use of millisecond spectroscopy as a simple and direct screen of the yield of B-branch electron transfer in large number of mutant complexes, allowing the complex femtosecond analysis to focus on mutants with an enhanced yield.

For B-branch electron transfer in the LM214H single mutant reaction centre a yield of $P^+H_B^-$ of 3–5% was estimated by Kirmaier and co-workers [41]. This is slightly lower than the present estimate of an 8% yield of $P^+Q_B^-$ in the WAAH complex. Possible reasons for this difference are additional effects of the Q_A-excluding AM260W mutation, and effects of the EL212A/DL213A mutation on electron transfer from H_B to Q_B. Regarding the AM260W mutation, it is known from the X-ray crystal structure that the protein structural changes resulting from this mutation are limited to the vicinity of the Q_A site, and that the mutation does not affect the rate of P* decay, both of which could be taken as evidence that the AM260W change is unlikely to affect the yield of B-branch electron transfer. However, the absence of Q_A means that the yield of the $P^+I_A^-\rightarrow$P* reaction is likely to be increased, which in principle would increase the possibility of an electron going down the B-branch. In addition, this mutation produces a small (2 nm) blue-shift of the P Q_y absorbance band, presumably through a protein structural change too subtle to be identified from the X-ray crystal structure (which had a resolution of 2.1 Å [49,62]). Taken together, these observations suggest that the Q_A-excluding AM260W mutation could increase the yield of B-branch electron transfer to a small extent.

Turning to the EL212A/DL213A mutation, this could affect the yield of the H_B^- to Q_B electron transfer step through an effect on the redox potential of Q_B/Q_B^-. In a previous study, we reported that the effect of this double mutation on the yield of B-branch electron transfer was variable, depending on which other mutations were also present [45]. At this stage it is unclear as to exactly whether or how this double mutation affects the yield of B-branch electron transfer in a background which has just the AM260W and LM214H mutations, and experiments to address this are planned.

Finally, there is also the issue of the effect of the environment of the reaction centre. Previous studies of the yield of B-branch electron transfer through ultrafast spectroscopy have used detergent-purified reaction centres, whereas the present study examined membrane-bound complexes by exploiting a strain of *R. sphaeroides* that lacks antenna complexes. One possibility, therefore, is that the higher yield of B-branch electron transfer seen in the WAAH reaction centre is due to the membrane environment. Certainly it is known that the membrane environment has small effects on the rate of A-branch electron transfer, with the rate of decay of the P* state being somewhat slower in membrane-bound reaction centres than in purified complexes [63,64]. An examination of the structure of the reaction centre shows that the accessory BChls in particular are quite solvent-exposed, which could make their electrochemical properties sensitive to the detergent and/or lipid environment. Another relevant factor is the occupancy of the Q_B site, which could be much higher in membrane-embedded reaction centres than in detergent-purified complexes, and which would obviously affect the yield of the H_B^- to Q_B step. Although we have not tested this explicitly, indications from both FTIR spectroscopy and millisecond time-scale transient absorbance spectroscopy are that the Q_B site is highly occupied in reaction centres embedded in antenna-deficient membranes [45–47].

Acknowledgement

This work was supported by the Netherlands Organization for Scientific Research (NWO) via the Dutch Foundation for Earth and Life Sciences (ALW) (DF, EGA and RVG), and the Biotechnology and Biological Sciences Research Council of the United Kingdom and the University of Bristol (MCW and MRJ). The authors wish to thank Prof. Peter Rich (University College London) for access to a single beam kinetic spectrophotometer and helpful discussions.

References

[1] J.P. Allen, G. Feher, T.O. Yeates, H. Komiya, D.C. Rees, Structure of the reaction center from *Rhodobacter sphaeroides* R-26: the protein subunits, Proc. Natl. Acad. Sci. U. S. A. 84 (1987) 6162–6166.

[2] C.H. Chang, O. El-Kabbani, D. Tiede, J. Norris, M. Schiffer, Structure of the membrane-bound protein photosynthetic reaction center from *Rhodobacter sphaeroides*, Biochemistry 30 (1991) 5352–5360.

[3] U. Ermler, G. Fritzsch, S.K. Buchanan, H. Michel, Structure of the photosynthetic reaction centre from *Rhodobacter sphaeroides* at 2.65 Å resolution: cofactors and protein–cofactor interactions, Structure 2 (1994) 925–936.

[4] U. Ermler, H. Michel, M. Schiffer, Structure and function of the photosynthetic reaction center from *Rhodobacter sphaeroides*, J. Bioenerg. Biomembranes 26 (1994) 5–15.

[5] J.P. Allen, G. Feher, T.O. Yeates, H. Komiya, D.C. Rees, Structure of the reaction center from *Rhodobacter sphaeroides* R-26: the cofactors, Proc. Natl. Acad. Sci. U. S. A. 84 (1987) 5730–5734.

[6] C. Kirmaier, D. Holten, W.W. Parson, Picosecond-photodichroism studies of the transient states in *Rhodopseudomonas sphaeroides* reaction centers at 5 kelvin: effects of electron transfer on the six bacteriochlorin pigments, Biochim. Biophys. Acta 810 (1985) 49–61.

[7] A.J. Hoff, J. Deisenhofer, Photophysics of photosynthesis. Structure and spectroscopy of reaction centers of purple bacteria, Phys. Rep. 287 (1997) 1–247.

[8] W.W. Parson, Reaction centers, in: H. Scheer (Ed.), Chlorophylls, CRC Press, Boca Raton, USA, 1991, pp. 1153–1180.

[9] G.R. Fleming, R. van Grondelle, The primary steps of photosynthesis, Phys. Today 47 (1994) 48–55.

[10] N.W. Woodbury, J.P. Allen, The pathway, kinetics and thermodynamics of electron transfer in wild type and mutant bacterial reaction centers of purple nonsulfur bacteria, in: R.E. Blankenship, M.T. Madigan, C.E. Bauer (Eds.), Anoxygenic Photosynthetic Bacteria, Kluwer Academic Publishing, Dordrecht, The Netherlands, 1995, pp. 527–557.

[11] W.W. Parson, Photosynthetic bacterial reaction centers, in: D.S. Bendall (Ed.), Protein electron transfer, BIOS Scientific, Oxford, UK, 1996, pp. 125–160.

[12] M.E. van Brederode, M.R. Jones, Reaction centres of purple bacteria, in: N.S. Scrutton, A. Holzenburg (Eds.), Enzyme-Catalysed Electron and Radical Transfer, Kluwer Academic/Plenum Publishers, New York, USA, 2000, pp. 621–676.

[13] M.Y. Okamura, M.L. Paddock, M.S. Graige, G. Feher, Proton and electron transfer in bacterial reaction centers, Biochim. Biophys. Acta, Bioenerg. 1458 (2000) 148–163.

[14] C.A. Wraight, Proton and electron transfer in the acceptor quinone complex of photosynthetic reaction centers from *Rhodobacter sphaeroides*, Front. Biosci. 9 (2004) 309–337.

[15] N. Ivashin, B. Kallenbring, S. Larsson, O. Hansson, Charge separation in photosynthetic reaction centers, J. Phys. Chem. 102 (1998) 5017–5022.

[16] M. Bixon, J. Jortner, M.E. Michel-Beyerle, A. Ogrodnik, A superexchange mechanism for the primary charge separation in photosynthetic reaction centers, Biochim. Biophys. Acta 977 (1989) 273–286.

[17] M.E. Michel-Beyerle, M. Plato, J. Deisenhofer, H. Michel, M. Bixon, J. Jortner, Unidirectionality of charge separation in reaction centers of photosynthetic bacteria, Biochim. Biophys. Acta 932 (1988) 52–70.

[18] M. Plato, K. Möbius, M.E. Michel Beyerle, M. Bixon, J. Jortner, Intermolecular electronic interactions in the primary charge separation in bacterial photosynthesis, J. Am. Chem. Soc. 110 (1988) 7279–7285.

[19] J. Hasegawa, H. Nakatsuji, Mechanism and unidirectionality of the electron transfer in the photosynthetic reaction center of *Rhodopseudomonas* viridis: SAC-CI theoretical study, J. Phys. Chem., B 102 (1998) 10420–10430.

[20] L.Y. Zhang, R.A. Friesner, *Ab initio* calculation of electronic coupling in the photosynthetic reaction center, Proc. Natl. Acad. Sci. U. S. A. 95 (1998) 13603–13605.

[21] D. Kolbasov, A. Scherz, Asymmetric electron transfer in reaction centers of purple bacteria strongly depends on different electron matrix elements in the active and inactive branches, J. Phys. Chem., B 104 (2000) 1802–1809.

[22] M. Ceccarelli, M. Marchi, Simulation and modeling of the *Rhodobacter sphaeroides* bacterial reaction center: structure and interactions, J. Phys. Chem., B 107 (2003) 1423–1431.

[23] M. Ceccarelli, M. Marchi, Simulation and modeling of the *Rhodobacter sphaeroides* bacterial reaction center: II. Primary charge separation, J. Phys. Chem., B 107 (2003) 5630–5641.

[24] M.A. Steffen, K. Lao, S.G. Boxer, Dielectric asymmetry in the photosynthetic reaction center, Science 264 (1994) 810–816.

[25] D. Frolov, A. Gall, M. Lutz, B. Robert, Structural asymmetry of bacterial reaction centers: a Qy resonant Raman study of the monomer bacteriochlorophylls, J. Phys. Chem., A 106 (2002) 3605–3613.

[26] M.R. Gunner, A. Nicholls, B. Honig, Electrostatic potentials in *Rhodopseudomonas viridis* reaction centers: implications for the driving force and directionality of electron transfer, J. Phys. Chem. 100 (1996) 4277–4291.

[27] W.W. Parson, Z.T. Chu, A. Warshel, Electrostatic control of charge separation in bacterial photosynthesis, Biochim. Biophys. Acta 1017 (1990) 251–272.

[28] M.A. Thompson, M.C. Zerner, A theoretical examination of the electronic structure and spectroscopy of the photosynthetic reaction center from *Rhodopseudomonas viridis*, J. Am. Chem. Soc. 113 (1991) 8210–8215.

[29] M. Marchi, J.N. Gehlen, D. Chandler, M. Newton, Diabatic surfaces and the pathway for primary electron transfer in a photosynthetic reaction center, J. Am. Chem. Soc. 115 (1993) 4178–4190.

[30] A. Warshel, Z.T. Chu, W.W. Parson, On the energetics of the primary electron-transfer process in bacterial reaction centers, J. Photochem. Photobiol. 82 (1994) 123–128.

[31] R.G. Alden, W.W. Parson, Z.T. Chu, A. Warshel, Calculations of electrostatic energies in photosynthetic reaction centers, J. Am. Chem. Soc. 117 (1995) 12284–12298.

[32] C. Kirmaier, D. Gaul, R. Debey, D. Holten, C.C. Schenck, Charge separation in a reaction center incorporating bacteriochlorophyll for photoactive bacteriopheophytin, Science 251 (1991) 922–927.

[33] B.A. Heller, D. Holten, C. Kirmaier, Control of electron-transfer between the L-side and M-side of photosynthetic reaction centers, Science 269 (1995) 940–945.

[34] P.D. Laible, C. Kirmaier, D. Holten, D.M. Tiede, M. Schiffer, D.K. Hanson, Formation of $P^+ Q_B^-$ via B-branch electron transfer in mutant reaction centres, in: G. Garab (Ed.), Photosynthesis: Mechanisms and Effects, Kluwer, Dordrecht, 1998, pp. 849–852.

[35] E. Katilius, T. Turanchik, S. Lin, A.K.W. Taguchi, N.W. Woodbury, B-side electron transfer in a *Rhodobacter sphaeroides* reaction center mutant in which the B-side monomer bacteriochlorophyll is replaced with bacteriopheophytin, J. Phys. Chem., B 103 (1999) 7386–7389.

[36] C. Kirmaier, D. Weems, D. Holten, M-side electron transfer in reaction center mutants with a lysine near the nonphotoactive B bacteriochlorophyll, Biochemistry 38 (1999) 11516–11530.

[37] C. Kirmaier, C.Y. He, D. Holten, Manipulating the direction of electron transfer in the bacterial reaction center by swapping Phe for Tyr near BChl(M) (L181) and Tyr for Phe near BChl(L) (M208), Biochemistry 40 (2001) 12132–12139.

[38] J.A. Roberts, D. Holten, C. Kirmaier, Primary events in photosynthetic reaction centers with multiple mutations near the photoactive electron carriers, J. Phys. Chem., B 105 (2001) 5575–5584.

[39] A.L. de Boer, S. Neerken, R. de Wijn, H.P. Permentier, P. Gast, E. Vijgenboom, A.J. Hoff, High yield of B-branch electron transfer in a quadruple reaction center mutant of the photosynthetic bacterium *Rhodobacter sphaeroides*, Biochemistry 41 (2002) 3081–3088.

[40] A.L. de Boer, S. Neerken, R. de Wijn, H.P. Permentier, P. Gast, E. Vijgenboom, A.J. Hoff, B-branch electron transfer in reaction centers of *Rhodobacter sphaeroides* assessed with site-directed mutagenesis, Photosynth. Res. 71 (2002) 221–239.

[41] C. Kirmaier, P.D. Laible, K. Czarnecki, A.N. Hata, D.K. Hanson, D.F. Bocian, D. Holten, Comparison of M-side electron transfer in *Rb. sphaeroides* and *Rb. capsulatus* reaction centers, J. Phys. Chem., B 106 (2002) 1799–1808.

[42] E. Katilius, Z. Katiliene, S. Lin, A.K.W. Taguchi, N.W. Woodbury, B side electron transfer in a *Rhodobacter sphaeroides* reaction center mutant in which the B side monomer bacteriochlorophyll is replaced with bacteriopheophytin: low-temperature study and energetics of charge-separated states, J. Phys. Chem., B 106 (2002) 1471–1475.

[43] C. Kirmaier, A. Cua, C.Y. He, D. Holten, D.F. Bocian, Probing M-branch electron transfer and cofactor environment in the bacterial photosynthetic reaction center by addition of a hydrogen bond to the M-side bacteriopheophytin, J. Phys. Chem., B 106 (2002) 495–503.

[44] P.D. Laible, C. Kirmaier, C.S.M. Udawatte, S.J. Hofman, D. Holten, D.K. Hanson, Quinone reduction via secondary B-branch electron transfer in mutant bacterial reaction centers, Biochemistry 42 (2003) 1718–1730.

[45] M.C. Wakeham, M.G. Goodwin, C. McKibbin, M.R. Jones, Photoaccumulation of the P^+ Q_B^- radical pair state in purple bacterial reaction centres that lack the Q_A ubiquinone, FEBS Lett. 540 (2003) 234–240.

[46] M.C. Wakeham, E. Nabedryk, J. Breton, M.R. Jones, Formation of a semiquinone at the Q_B site by A-branch or B-branch electron transfer in the reaction centre from *Rhodobacter sphaeroides*, Biochemistry 43 (2004) 4755–4763.

[47] J. Breton, M.C. Wakeham, P.K. Fyfe, M.R. Jones, E. Nabedryk, Characterization of the bonding interactions of Q_B upon photoreduction via A-branch or B-branch electron transfer in mutant reaction centers from *Rhodobacter sphaeroides*, Biochim. Biophys. Acta, Bioenerg. 1656 (2004) 127–138.

[48] J.P. Ridge, M.E. van Brederode, M.G. Goodwin, R. van Grondelle, M.R. Jones, Mutations that modify or exclude binding of the Q_A ubiquinone and carotenoid in the reaction center from *Rhodobacter sphaeroides*, Photosynth. Res. 59 (1999) 9–26.

[49] K.E. McAuley, P.K. Fyfe, J.P. Ridge, R.J. Cogdell, N.W. Isaacs, M.R. Jones, Ubiquinone binding, ubiquinone exclusion, and detailed cofactor conformation in a mutant bacterial reaction center, Biochemistry 39 (2000) 15032–15043.

[50] D.K. Hanson, L. Baciou, D.M. Tiede, S.L. Nance, M. Schiffer, P. Sebban, In bacterial reaction centers protons can diffuse to the secondary quinone by alternative pathways, Biochim. Biophys. Acta 1102 (1992) 260–265.

[51] D.K. Hanson, D.M. Tiede, S.L. Nance, C.-H. Chang, M. Schiffer, Site-specific and compensatory mutations imply unexpected pathways for proton delivery to the Q_B binding-site of the photosynthetic reaction-center, Proc. Natl. Acad. Sci. U. S. A. 90 (1993) 8929–8933.

[52] P. Maróti, D.K. Hanson, L. Baciou, M. Schiffer, P. Sebban, Proton conduction within the reaction centers of *Rhodobacter-capsulatus*—the electrostatic role of the protein, Proc. Natl. Acad. Sci. U. S. A. 91 (1994) 5617–5621.

[53] M.R. Jones, G.J.S. Fowler, L.C.D. Gibson, G.G. Grief, J.D. Olsen, W. Crielaard, C.N. Hunter, Construction of mutants of *Rhodobacter sphaeroides* lacking one or more pigment–protein complexes and complementation with reaction-centre, LH1, and LH2 genes, Mol. Microbiol. 6 (1992) 1173–1184.

[54] M.R. Jones, M. Heer-Dawson, T.A. Mattioli, C.N. Hunter, B. Robert, Site-specific mutagenesis of the reaction centre from *Rhodobacter sphaeroides* studied by Fourier transform Raman spectroscopy: mutations at tyrosine M210 do not affect the electronic structure of the primary donor, FEBS Lett. 339 (1994) 18–24.

[55] C.C. Gradinaru, I.H.M. van Stokkum, A.A. Pascal, R. van Grondelle, H. van Amerongen, Identifying the pathways of energy transfer between carotenoids and chlorophylls in LHCII and CP29: a multicolor, femtosecond pump-probe study, J. Phys. Chem., B 104 (2000) 9330–9342.

[56] M.C. Wakeham, D. Frolov, P.K. Fyfe, R. van Grondelle, M.R. Jones, Acquisition of photosynthetic capacity by a reaction centre that lacks the Q_A ubiquinone; possible insights into the evolution of reaction centres? Biochim. Biophys. Acta, Bioenerg. 1607 (2003) 53–63.

[57] I.H.M. van Stokkum, T. Scherer, A.M. Brouwer, J.W. Verhoeven, Conformational dynamics of flexibly and semirigidly bridged electron donor–acceptor systems as revealed by spectrotemporal parametrization of fluorescence, J. Phys. Chem. 98 (1994) 852–866.

[58] M.E. van Brederode, F. van Mourik, I.H.M. van Stokkum, M.R. Jones, R. van Grondelle, Multiple pathways for ultrafast transduction of light energy in the photosynthetic reaction centre of *Rhodobacter sphaeroides*, Proc. Natl. Acad. Sci. U. S. A. 96 (1999) 2054–2059.

[59] C. Kirmaier, P.D. Laible, D.K. Hanson, D. Holten, B-side charge separation in bacterial photosynthetic reaction centers: nanosecond time scale electron transfer from H_B^- to Q_B, Biochemistry 42 (2003) 2016–2024.

[60] W.W. Parson, R.J. Cogdell, The primary photochemical reaction of bacterial photosynthesis, Biochim. Biophys. Acta 416 (1975) 105–149.

[61] W.W. Parson, R.K. Clayton, R.J. Cogdell, Excited states of photosynthetic reaction centers at low redox potentials, Biochim. Biophys. Acta 387 (1975) 265–278.

[62] K.E. McAuley, P.K. Fyfe, J.P. Ridge, N.W. Isaacs, R.J. Cogdell, M.R. Jones, Structural details of an interaction between cardiolipin and an integral membrane protein, Proc. Natl. Acad. Sci. U. S. A. 96 (1999) 14706–14711.

[63] S. Schmidt, T. Arlt, P. Hamm, C. Lauterwasser, U. Finkele, G. Drews, W. Zinth, Time-resolved spectroscopy of the primary photosynthetic processes of membrane-bound reaction centers from an antenna-deficient mutant of *Rhodobacter capsulatus*, Biochim. Biophys. Acta 1144 (1993) 385–390.

[64] L.M.P. Beekman, R.W. Visschers, R. Monshouwer, M. Heer-Dawson, T.A. Mattioli, P. McGlynn, C.N. Hunter, B. Robert, I.H.M. van Stokkum, R. van Grondelle, M.R. Jones, Time-resolved and steady-state spectroscopic analysis of membrane-bound reaction centers from *Rhodobacter sphaeroides*. Comparisons with detergent-solubilized complexes, Biochemistry 34 (1995) 14712–14721.